Arabian Journal of Chemistry (2021) **14**, 103110

King Saud University

**Arabian Journal of Chemistry**

www.ksu.edu.sa
www.sciencedirect.com

ORIGINAL ARTICLE

# Synthesis of silver nanoparticles using root extract of *Duchesnea indica* and assessment of its biological activities

**Ihsan Ilahi [a], Fazli Khuda [a,*], Muhammad Umar Khayam Sahibzada [b,*], Saad Alghamdi [c], Rahim Ullah [a], Zakiullah [a], Anas S. Dablool [d], Mehboob Alam [e], Ayub Khan [f], Atif Ali Khan Khalil [g]**

[a] *Department of Pharmacy, University of Peshawar, Peshawar, Khyber Pakhtunkhwa, Pakistan*
[b] *Department of Pharmacy, Sarhad University of Science and Information Technology, Peshawar, Khyber Pakhtunkhwa, Pakistan*
[c] *Laboratory Medicine Department, Faculty of Applied Medical Sciences, Umm Al-Qura University, P.O.Box. 715, Makkah, 21955, Saudi Arabia*
[d] *Department of Public Health, Health Sciences College at Al-Leith, Umm Al-Qura University, Makkah, Saudi Arabia*
[e] *Department of Pharmacy, Capital University of Science and Technology, Islamabad, Pakistan*
[f] *Department of Chemistry, University of Education, Jauharabad Campus, Lahore, Pakistan*
[g] *Department of Biological Sciences, National University of Medical Sciences, Rawalpindi, Pakistan*

Received 13 January 2021; accepted 28 February 2021

**KEYWORDS**

*Duchesnea indica*;
Silver nanoparticles;
Characterization;
Biological activities

**Abstract** Treatment of microbial infections and inflammatory conditions have many challenges in terms of efficacy and safety issues. Novel approaches such as nanoparticles based drug delivery system have shown promising results to solve some of these problems. The aim of this study was to exploit the efficacy of the synthesized silver nanoparticles. In this study, silver nanoparticles (AgNPs) were biosynthesized using root extract (aqueous) of *Duchesnea indica*. They were characterized using different techniques such as, ultraviolet–visible (UV–Vis) spectrophotometry, transmission and scanning electron microscopy (TEM and SEM), X-ray diffractometer (XRD), energy dispersive X-ray spectroscopy (EDX), fourier-transform infrared spectroscopy (FTIR) and zetasizer. The UV–Vis spectra gave a characteristic peak at 423 nm; XRD confirmed its crystalline structure; FTIR confirmed the involvement of phytochemicals in their capping and reduction; TEM images confirmed their spherical shape with average width of 20.49 nm and average area of 319.25 $nm^2$. Various biological activities were performed on these NPs, such as antimicro-

* Corresponding authors.
E-mail addresses: fazlikhuda@uop.edu.pk (F. Khuda), umar.sahibzada@gmail.com (M. Umar Khayam Sahibzada).
Peer review under responsibility of King Saud University.

Production and hosting by Elsevier

https://doi.org/10.1016/j.arabjc.2021.103110

bial, anti-inflammatory, analgesic and muscle relaxant, which showed significant results as follow. Among bacterial strains, *Salmonella typhi* (MIC: 0.01 mg/ml) and *Escherichia coli* (MIC: 0.01 mg/ml), while among that of fungal *Microsporum canis* (MIC: 0.53 mg/ml) and *Alternaria alternata* (MIC: 0.51 mg/ml) were most susceptible. The AgNPs showed maximum anti-inflammatory activity (46.15 and 56.85%) at 20 mg/kg after 3 and 5 h of drug administration, comparable to that of standard. *In-vivo* model exhibited concentration dependent inhibition of both *COX-2* and *5-LOX* enzymes. Similarly, it exhibited maximum analgesic activity (54.24%) at 20 mg/kg dose after 60 min. of pain induction. Furthermore, they depicted maximum muscle relaxation ($P < 0.01$) after 60 and 90 min of drug administration. Above results suggest that these AgNPs can be studied further for the development of more effective and safe formulations.



## 1. Introduction

Nanotechnology is a rapidly expanding area of research concerned with the study of particles ranging from about 1–100 nm (Mathew et al., 2020; Nandini et al., 2020). Metallic nanoparticles (NPs) has a widespread practical applications in areas such as targeted drug delivery, magnetic resonance imaging, vaccine administration, biomedicines, drug-gene delivery, cosmetics, biomedical sciences, optoelectronics and catalysis (Oprica et al., 2020; Patil, 2020; Rana et al., 2020; Sharma et al., 2021).

Green synthesis of metallic NPs is an important area of nano research. This approach utilizes eco-friendly, nontoxic stabilizing and reducing agents for the synthesis of NPs. In contrast, conventional physical and chemical methods generate a large amount of toxic by-products (Ponsanti et al., 2020).

Different biological agents derived from plants, microorganisms and enzymes have been widely reported for the synthesis of metallic NPs. Among plants, *Eucalyptus globules*, *Abelmoschus esculentus, Cleome viscosa*, *Nerium oleander* and *Gymnocladus assamicus* etc. based NPs have shown significant antifungal, antioxidant and catalytic activities (Ahmad et al., 2020). Similarly, eukaryotic organisms such as fungi have got considerable attention for synthesis of NPs. These organisms secret different enzymes that acts as catalyst in capping and reduction of metallic NPs. It has been reported that microbial based NPs particularly those derived from higher fungi (basidiomycete) are very effective in combating plant pathogens such as *Pyricularia grisea*, *Sclerospora graminicola, Colletotrichum capsici* and *Phytophthora* infestans (Jogaiah et al., 2019; Joshi et al., 2021). More recently, secretomic-based nanoparticles have been studied for heavy metal detoxification, CNS disorders and in the treatment of cancer (Geetha et al., 2021).

Plant based synthesis of silver NPs (AgNPs) could be more advantageous over other methods such as the lessening of biohazards, depletion of the cost of microorganism isolation and its culture media and elimination of complicated process of maintaining cell cultures. Furthermore, these NPs are more stable with no aggregation problems. Similarly, plants contains several biomolecules such as flavonoids and phenols that play a significant role in fast bioreduction of Ag ions (Lim et al., 2020; Tailor et al., 2020).

*Duchesnea indica* (Andr.) Focke (*D. indica*) is a perineal herb, belongs to the family Rosaceae and is widely distributed China, India and Pakistan. Several phytochemicals, including flavonoids, sterols, triterpenes, polyphenols and volatile oils are present in this plant (Qiao et al., 2009). Traditionally, this plant has been used in the treatment of many diseases such as cancer, fever, inflammation and various skin disorders (Hu et al., 2011; Luo et al., 2020; Yang et al., 2019). Due to its diverse therapeutic activities, synthesis of AgNPs from the root extract of this plant may enhance its safety and efficacy. AgNPs itself possess antimicrobial properties, therefore they are of interest and can be utilized into antimicrobial, cosmetic and skin products (Al-Radadi, 2019; Oves et al., 2015).

In present study, we explored the therapeutic applications of AgNPs derived from *D. indica* crude extract. The extract was selected on the basis of its traditional uses in ayurvedic medicines. Initially, the crude extract was screened for antimicrobial, anti-inflammatory, analgesic and muscle relaxant properties. The crude extract depicted significant results in both *In-vivo* and *In-vitro* models. Therefore, the said extract was further selected for the synthesis of AgNPs with the aim to formulate more effective and safe therapy.

The resulting NPs were then characterized using different techniques such as UV– visible spectroscopy (UV–Vis), scanning and transmission electron microscopy (SEM and TEM), Fourier transform infra-red spectroscopy (FTIR), X-ray diffractometer (XRD), energy dispersive X-ray spectroscopy (EDX) and Zetasizer. The effect of temperature, pH and substrate concentration on the production of AgNPs were also studied. Moreover, the synthesized AgNPs were screened for its antimicrobial, anti-inflammatory, analgesic and muscle relaxant activities.

## 2. Material and methods

### 2.1. Plant material

*D. indica* roots were collected from Galyat (Bara Gali), Pakistan (Specimen number: 10708 BOT). The roots were thoroughly washed with fresh deionized water, dried in shade and subsequently crushed into coarse powder.

### 2.2. Preparation of aqueous root extract

Approximately 50 g o the powdered material was added to distilled water (300 ml) and heated at 50 to –60 °C for about 50 min. The solution was then allowed to cool at room temperature. The resulting aqueous extract was stirred at 400 rpm for

1.5 h at room temperature and subsequently centrifuged (6000 rpm) for 10 min. in order to separate undesirable impurities. Finally, the supernatant was passed through Whatman No. 1 filter paper and the clear filtrate was stored at 4 °C (Ahmad et al., 2017) until used.

### 2.3. Synthesis of AgNPs

For the synthesis of AgNPs, 10 ml of root extract was mixed with 90 ml (2 mM) of aqueous silver nitrate ($AgNO_3$) solution. The resulting solution was thoroughly stirred using a magnetic stirrer (350 rpm) at 25 °C for about 1 h. After mixing the extract with silver nitrate solution, the color of the mixture rapidly changed from light-green to yellowish-brown, thereby indicating the reduction of Ag ions to AgNPs. This solution was then incubated for 24 h (37 °C) for maximum production of AgNPs. The bioreduction of Ag ions was further monitored by U.V-Vis spectral analysis at a wavelength between 350 and 800 nm (Algebaly et al., 2020).

### 2.4. Purification of AgNPs

The colloidal dispersion was centrifuged (12,000 rpm) for 10 min; the supernatant was discarded and the pellets were washed with deionized water to remove free ions and any unreacted moieties. This was followed by washing with distilled ethanol. The AgNPs were then dried using a benchtop freeze drier and were stored at 25 °C for further use (Ahmad, et al., 2017).

### 2.5. Characterization of AgNPs

The synthesis of AgNPs was confirmed by UV–Vis spectrophotometer (Perkin-Elmer, Lamda 35, Germany) via analysing the Surface plasmon resonance (SPR). The surface morphologies were analysed by TEM (Hitachi-7650) and SEM (S-2500, Japan) techniques. The crystalline nature of NPs was investigated using XRD (Japan, model JDX-3532 JEOL) at $\lambda = 1.5406$ A° with Cu Kα irradiation line. FTIR spectroscopy (Perkin-Elmer, Spectrum Version 10.5.1) was used to analyse different moieties that may be involved in the synthesis and stabilization of AgNPs. The EDX (NOVA-450 instrument) and Zetasizer were used to analyse the elemental composition and zeta potential of AgNPs, respectively.

### 2.6. Optimization and stability of AgNPs

The effect of substrate concentration on the production of AgNPs was evaluated at different ratio of $AgNO_3$ while keeping the volume of *D. indica* root extract constant (1:5, 1:9, 1:13, and 1:17 v/v, respectively). The optimum concentration for the synthesis of AgNPs was confirmed by *UV–Vis* spectroscopy. Optimization studies with respect to temperature were carried out by reacting plant extract and $AgNO_3$ at temperature ranging from 30 °C to 80 °C. For pH optimization, AgNPs were dispersed in phosphate buffer solution at variable pH, ranging from 3, 6, 7, 8, and 12. Furthermore, the stability of AgNPs were assessed between 350 nm and 800 nm at different time intervals such as 15, 30 and 60 days (Islam et al., 2019).

### 2.7. Biological activities of synthesized AgNPs

#### 2.7.1. Antimicrobial activities

"Well diffusion" method was adopted for the evaluation of both antibacterial and antifungal activities (Boyanova et al., 2005). The following bacterial strains were used in the study. *Klebsiella pneumonia* (ATCC 700603), *Salmonella typhi* (ATCC 19430), *Salmonella enteritidis* (ATCC 13076), *Pseudomonas aeruginosa* (ATCC 27853), *Escherichia coli* (ATCC 5922), *Shigella flexneri* (ATCC 29903), *Staphylococcus aureus* (ATCC 25923), *Bacillus subtilis* (ATCC 6633) and *Staphylococcus epidermidis* (ATCC 12228). The antifungal activity was carried using the fungal strains; *Alternaria alternata* (ATCC 96154), *Microsporum canis* (ATCC 11622), *Aspergillus flavus* (ATCC 32611), *Candida albicans* (ATCC 2091), *Aspergillus niger* (ATCC 10549), *Aspergillus terreus* (ATCC 20542), *Fusarium solani* (ATCC 11712), *Candida glabrata* (ATCC 90030), and *Trichophyton longifusis* (Clinical isolate). The studied microbial strains were obtained from the Department of biotechnology, University of Peshawar. Imipenem and Miconazole were used as positive controls. The MIC of AgNPs against susceptible microbial strains were determined by micro dilution method (Punjabi et al., 2018). The bioassays were performed in triplicate.

#### 2.7.2. Animals

Healthy BALB/c mice of both sex (25–30 g) were used in this assay. The animals were housed in metal cages under standard environmental conditions i.e. 22 ± 2 °C and 12 hrs light/dark cycle; for at least one week. The experimental animals had free access to food and water (*ad libitum*). Study was approval by the *Ethical Committee of* "Faculty of life and environmental sciences, University of Peshawar" under applicant number 08/EC/F.LIFE-2020.

#### 2.7.3. Anti-inflammatory activity

*2.7.3.1. In-vivo carrageenan- induced hind paw edema model.* This activity was conducted using a well-established procedure (Lingadurai et al., 2007). Animals were divided into eight groups. Each group was consist of five animals ($n = 5$). Animals in group I did not received the drug and served as negative control while those in group II were administered with Diclofenac as standard (20 mg/kg) and served as positive control. Likewise, those in groups III, IV and V were given AgNPs at different doses (5, 10 and 20 mg/kg, respectively) while those in groups VI, VII and VIII were administered with crude drug (50, 100 and 200 mg/kg, respectively). Both the extract and AgNPs were administered intraperitoneally (*ip*).

After 30 min of treatment, they were injected with carrageenan (0.05 ml; 1%) solution via subplantar region of the left hind paw. The circumference of the hind paw was measured at different time intervals (0, 1, 2, 3, and 5 hrs) using digital plethysmometer (Plan lab, Spain). Percentage inhibition was measured from Eq. (1).

$$\%\ Inhibition = \left(\frac{C - T}{C}\right) \times 100 \quad (1)$$

where C and T are the increase in paw volume of control and test treatment groups, respectively.

*2.7.3.2. In-vitro cyclooxygenase (COX-2) assay*. The COX-2 assay was performed following reported method with minor modifications (Olomola et al., 2020). Purified COX-2 enzyme was purchased from Sigma-Aldrich. The enzyme (300 U/ml) was activated with 50 µl of co-factor solution on ice for 5 to 10 min. Likewise, enzyme-solution (60 µl) and AgNPs (20 µl) or crude extract (31.25–1000 µg/mL) were mixed and allowed to stand at 25 °C for 5 min; followed by addition of 20 µl arachidonic acid (30 mM). The mixture was then incubated at 37 °C for 5 min. Maximum absorbance (570 nm) was measured with *UV–Vis* spectrophotometer. The percent inhibition was calculated and $IC_{50}$ values were determined.

*2.7.3.3. In-vitro 5-lipoxygenase (5-LOX) assay*. Various concentrations of AgNPs and /or crude extract (31.25–1000 µg/ml), 5-LOX enzyme (10,000 U/ml) and phosphate buffer solutions (50 mM; pH 6.3) were prepared. The LOX enzyme (250 µl), phosphate buffer (250 µl) and AgNPs and /or crude extract (31.25–1000 µg/ml) solutions were mixed and incubated for 5 min at 25 °C. I ml of substrate solution (Linoleic-acid; 0.6 mM) was then mixed with enzyme solution and after further incubation (25 °C) for 5 min. maximum absorbance (234 nm) was measured (Okur et al., 2021). The percent inhibition was measured from Eq. (2).

$$\text{Percent Inhibition} = \frac{\text{Control Absorbance} - \text{Sample Absorbance}}{\text{Control Absorbance}} \times 100 \quad (2)$$

*2.7.4. Analgesic activity*

The analgesic activity was determined using hot plate method (54 ± 0.1 °C) (Winter et al., 1962). Healthy BALB/c mice (either sex; weight 20 g) were used in the assay. The experimental animals were randomly divided into eight groups. Each group was consist of five animals ($n = 5$). Animals in group-I received normal saline (NS) while those in group-II were given Tramadol (30 mg/kg) and served as negative and positive controls, respectively. Likewise, those in groups III, IV and V were given AgNPs at different doses (5, 10 and 20 mg/kg, respectively) while those in groups VI, VII and VIII were administered with crude drug (50, 100 and 200 mg/kg, respectively). The standard, crude and AgNPs were given *ip*.

After 30 min. of drug administration, all the animals were exposed to hot plate at 54 °C and pain responses such as flicking, licking and jumping were recorded after each 30 min. The overall study was conducted for 90 min duration; the baseline latencies were performed for 30 s. Percentage protection (PT) was calculated using Eq. (3).

$$PT = \left(\frac{Tl - Cl}{Ct - Cl}\right) \times 100 \quad (3)$$

where *Tl*: test latency; *Cl*: control latency and Ct: cut off time.

*2.7.5. Muscle relaxant activity*

*2.7.5.1. Traction test*. This test was performed using a rubber coated metallic wire. It was supported with stands about 30 cm above the laboratory bench. The animals were divided into different groups ($n = 5$). Animals in group-I were given NS (10 ml/kg) while those in group-II were treated with standard diazepam (0.25 mg/kg) and served as negative and positive control, respectively. The remaining groups received aqueous extract (50, 100 and 200 mg/kg) and AgNPs (5, 10 and 20 mg/kg). All the drugs were administered *ip*. The animals were screened at different time intervals (30, 60 and 90 min) after treatment with normal saline, standard, AgNPs and plant extract. The animals were hanged from hind legs for five seconds and the failure to hang for the said duration was considered as the presence of studied activity (Villar et al., 1992).

*2.7.5.2. Chimney test*. The experiment was conducted using a well-established method with slight modification (Biziere et al., 1987). This test was performed using a pyrex glass tube (length 30 cm; diameter 3 cm) having a mark at 20 cm from the base. The animals were grouped and dosed in the same manner as described in the traction test. The animals were allowed to move towards the designated mark from one end of the tube and when they reached that mark, the tube was immediately turned into a vertical position. The time required by each animal to climb back to its original position was noted. The animal failed to reach to the designated mark within 30 s was considered with relaxed muscles.

*2.8. Statistical analysis*

Statistical analysis were performed using one-way ANOVA. This was followed by Dunnet post hoc test. (GraphPad Software Inc. San Diego CA, USA). Results were expressed as mean ± SEM.

## 3. Results and discussion

*3.1. Synthesis of AgNPs*

The color of the aqueous root extract was changed from light-green to yellowish-brown upon the addition of 2 mM $AgNO_3$ solution from 30 min to 1 h. No change in color was observed up to 24 h of incubation. This indicates the presence of high concentration of flavonoids, phenols and other phytochemicals which might be involved in the bioreduction of Ag to AgNPs. Several other reports have also confirmed the same (Ahmad, et al., 2020). This method is comparatively simple, rapid as well as safe, as it does not require the use of hazardous chemical substances.

*3.2. Characterization of AgNPs*

*3.2.1. UV–Vis analysis*

The UV-absorption spectra of the plant extract and AgNPs are shown in Fig. 1A. The wavelength was fixed between 350 and 800 nm. The characteristic peak for AgNPs was located at 423 nm, corresponding to the surface plasmon resonance of AgNPs.

*3.2.2. SEM and TEM analysis*

The microstructures and surface characteristics of AgNPs were obtained from SEM and TEM images. The SEM image (Fig. 2A) indicates that the synthesized AgNPs have certain degree of agglomeration. Furthermore, the TEM images (Fig. 2B, 2C & 2D) confirmed that the AgNPs predominantly grow in spherical shape with average width of 20.49 nm (Fig. S1A) and average area of 319.25 $nm^2$ (Fig. S1B). The

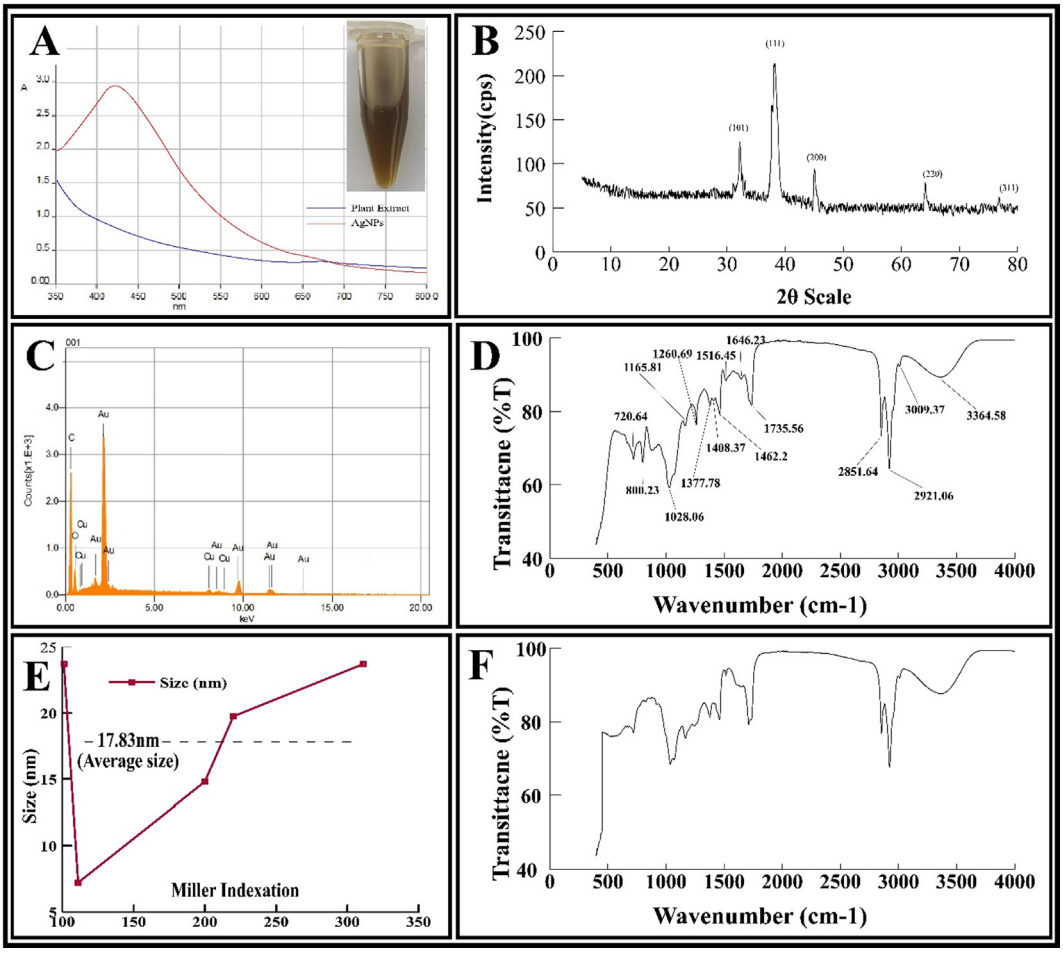


**Fig. 1** (A) UV–visible spectra, (B) energy dispersive diagram, (C) XRD pattern, (D) FT-IR spectrum of AgNPs, (E) Average size calculation of AgNPs using Debye-Scherrer's size approximation formula and (F) FT-IR spectrum of aqueous root extract.

presence of small and large NPs were due to the formation of AgNPs in early and later stages of the reaction, which indicates that both nucleation and aggregation happened consecutively.

### 3.2.3. EDS analysis

The EDS analysis was conducted to confirm the presence of Ag, C and O in AgNPs (Fig. 1B). There were no other peaks in the EDS spectrum, which showed high purity of synthesized AgNPs.

### 3.2.4. XRD analysis

The XRD patterns (Fig. 1C) show the characteristic peaks for AgNPs at 2θ values of 31.9°, 37.9°, 44.8°, 65.1°, and 77.2°. These values are assigned to 101, 111, 200, 220, and 311 plain of the face centred cubic structure of NPs (JCPDS file: 04-0783). The sharp peak located at 38.2° indicated its ultra-fine nature. The mean crystallite size of AgNPs was calculated as 20.39 nm, using Debye-Scherrer's equation (Eq.4).

$$D(nm) = \left(\frac{0.9\lambda}{\beta\cos\theta}\right) \quad (4)$$

where D: mean crystal size, λ: wavelength of X-ray and β: full-width at half maximum of the XRD peak at the diffraction angle θ.

Graphical representation of Average size calculation using Scherer size approximation formula is shown in Fig. 1E.

### 3.2.5. FT-IR spectroscopy analysis

Fig. 1D and 1F represents the FT-IR spectrum of AgNPs and plant extract, respectively. The spectra of extract shows different stretching vibrations pattern of functional groups after binding to Silver ions. The spectra reveals that these functional groups play a crucial role in stabilizing and capping the metallic ions ($Ag^+$). The bands at 3364.58 $cm^{-1}$ are due to hydroxyl groups (–OH). Similarly, the various bands at 2851.64, 2921.06 and 3009.37 $cm^{-1}$ corresponds to –CH stretching. Two peaks at 1260.69 and 1735.56 $cm^{-1}$ corresponds to C–O stretching of the ester functional groups. The band at 1646.23 $cm^{-1}$ shows the existence of carbonyl functional group (C = O). Similarly, the bands at 1516.45, 1462.2, 1408.37, 1377.78, 1165.81, and 1028.06 $cm^{-1}$, correspond to the amide II (N–H) group, methylene group ($–CH_2$), phenolic –OH group, N–O group, C-O-C stretching, and C–N stretching vibration of amine, respectively.

### 3.2.6. Zeta potential and zeta size analysis

The zeta potential and size of AgNPs was determined by Zetasizer (Malvern). The zeta potential (Fig. S1C) and the zeta size

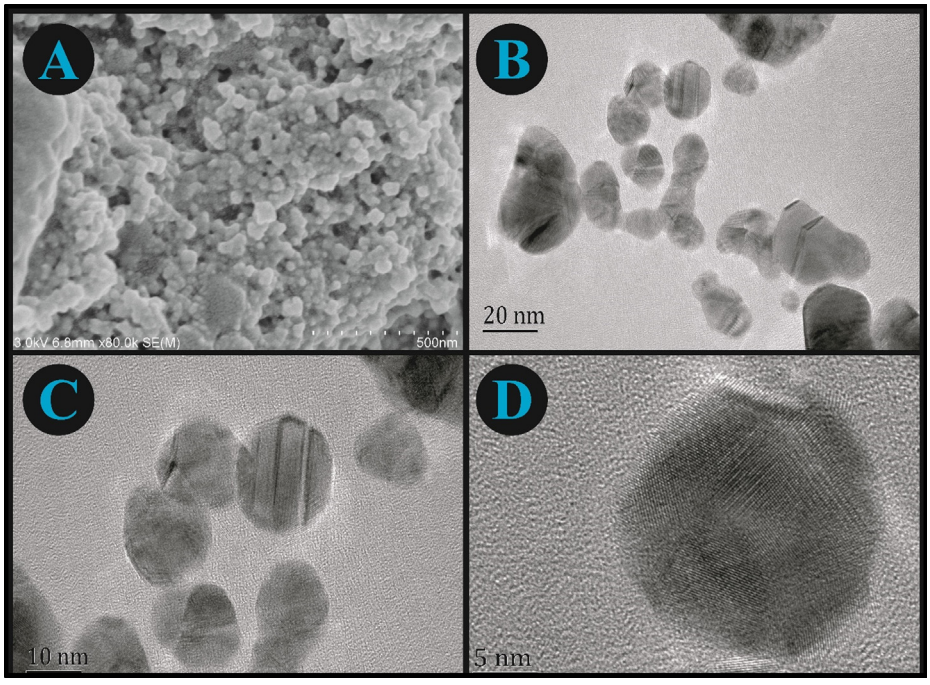


**Fig. 2** (A) SEM and TEM (B, C, and D) results of AgNPs at different resolutions.

(Fig. S1D) for AgNPs was found to be −21.3 mV and 54 nm, respectively.

### 3.3. Optimization and stability of AgNPs

Different ratios of aqueous extract and $AgNO_3$ (1:5, 1:9, 1:13 and 1:17 v/v, respectively) were used to obtain the higher yield of AgNPs. Optimum synthesis took place at 1:9 v/v concentration of $AgNO_3$ with maximum absorption observed at 422.26 nm (Fig. 3A). The effect of varying temperature on the production of AgNPs was studied at different temperature from 30 °C to 80 °C. The maximum absorption peak (433 nm) was observed at 80 °C, which indicates the highest production of AgNPs at this temperature (Fig. 3B). The pH range of 3.0, 6.0, 7.0, 8.0 and 12.0 were chosen for assessing the stability of AgNPs. The SPR peaks were relatively stable at neutral and basic pH. Whereas, it diminished at acidic pH (Fig. 3C). It indicates that the synthesis of AgNPs is facilitated by alkaline pH. Also, in basic pH, the NPs dispersion retained their characteristic yellowish-brown color, however a change in color was observed as the pH becomes more acidic. The stability of synthesized AgNPs was observed for 2 months at intervals of 15, 30, and 60 days, respectfully. The SPR peaks revealed high stability of AgNPs for 60 days study duration (Fig. 3D).

### 3.4. Antibacterial activity

The antibacterial properties of crude extract, AgNPs and standard were tested against different bacterial strains (Fig. S2 & Table 1).

Although it showed activity against all bacterial strains tested, however, it was more effective against *S. typhi* and *S. epidermidis* showing highest zone of inhibition (29 mm each; MIC 0.01). *E. coli, S. enteritidis* and *S. flexneri* were among the other susceptible strains showed 25, 22 and 21 mm zone of inhibition (MIC: 0.01, 0.01, 0.1), respectively. These pathogenic strains cause various infectious diseases like typhoid, diarrhoea and other infections. Crude extract of the study plant has already been reported in western herbalism for the treatment of various infections, mostly caused by the above mentioned strains (Hu, et al., 2011; Luo, et al., 2020). The use of AgNPs can potentiate the activity of plant extracts thereby reducing the dose, and side effects (Robles-Martínez et al., 2019). Present study suggests the possibility of using AgNPs against these bacterial strains.

Possible mechanisms for its activity, as reported by previous studies may include, but not limited to, penetration into the cell wall; generation of free radicals causing increased cell membrane porosity; inactivation of enzymes by conjugation of sulfhydryl groups; and DNA damage (Feng et al., 2000; Sondi, and Salopek-Sondi, 2004). However further studies are required to elucidate the exact mechanism (s) for the same.

### 3.5. Antifungal activity

Among dermatophytes, *D. indica* derived AgNPs showed highest percent inhibition (90, 80 and 75%) against *M. canis, A. alternata* and *F. solani,* respectively as compared to standard (Fig. S3A & Table 2).

Crude extract showed maximum inhibition (50% each) against *A. alternata* and *M. canis*. Also, *D. indica* root extracts had previously shown significant activity against *M. canis* and *F. solani* (Fazli et al., 2012). Similarly, the extract is famous for the treatment of skin related disorders as well. In addition, silver itself possess potential antifungal activity (Hu, et al., 2011). Therefore, this added advantage greatly promotes the use of AgNPs as alternative herbal therapy for the effective treatment of skin related disorders. Fig. S3B shows a comparison between percent inhibition of miconazole, crude extract and AgNPs against different fungal strains.

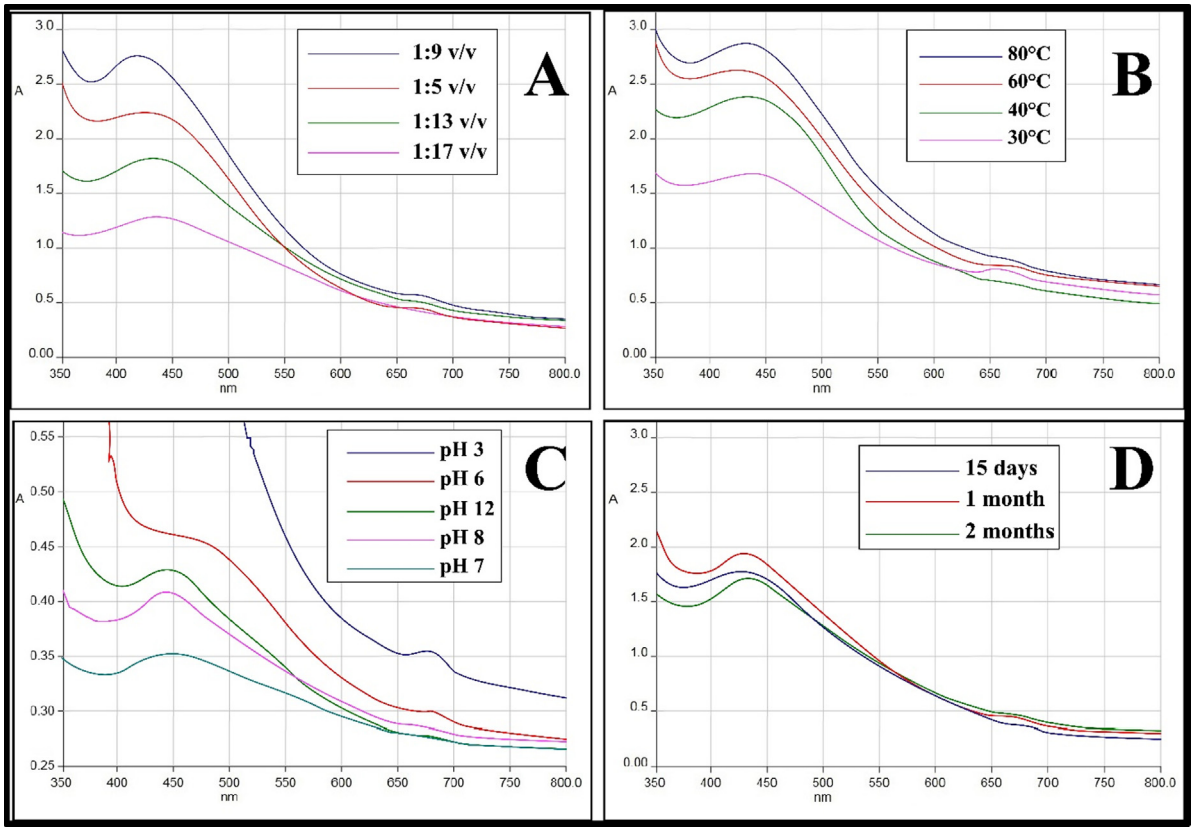


**Fig. 3** (A) UV–Vis absorption spectra of AgNPs at different concentration of $AgNO_3$; (B) temperature; (C) pH and (D) at different time interval.

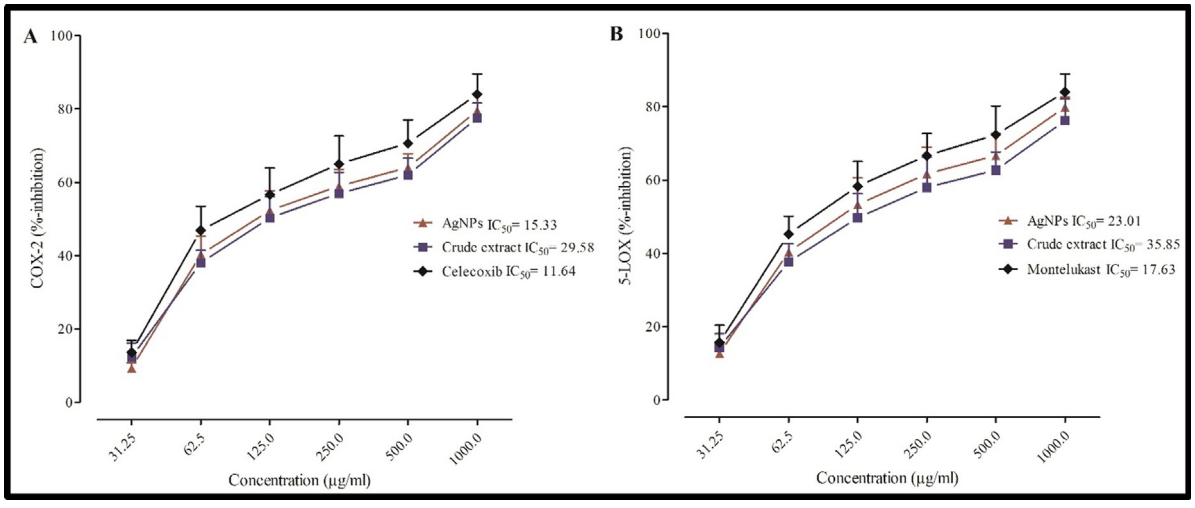


**Fig. 4** The relative inhibition of (A) COX-2 and (B) 5-LOX enzymes by crude extract, AgNPs and standard.

### *3.6. Anti-inflammatory activity*

#### *3.6.1. In-vivo carrageenan- induced hind paw edema model*

*D. indica* is well known for anti-inflammatory activity due to the presence of different phytochemicals such as phenolic acids and flavonoids, which have potent anti-inflammatory properties (Fazli et al., 2014; Zhao et al., 2008). AgNPs at 20 mg/kg exhibited significant ($P < 0.001$) anti-inflammatory activity comparable to that of standard (Table 3). The maximum inhibition (46.15 and 56.85%) was observed at 20 mg/kg dose after 3 and 5 h of drug administration while the standard showed 61.46 and 71.54% inhibition at the same dose. Similarly,

**Table 1** IZ and MIC of extract, AgNPs and standard against different bacterial strains.

| Test microorganisms | Crude extract | | AgNPs | | Imipenem | |
|---|---|---|---|---|---|---|
| | IZ | MIC | IZ | MIC | IZ | MIC |
| *Bacillus subtilis* | – | – | 15 | 0.08 | 35 | 0.0003 |
| *Escherichia coli* | 12 | 0.71 | 25 | 0.01 | 32 | 0.0002 |
| *Klebsiella pneumonia* | 8 | 0.82 | 15 | 0.06 | 15 | 0.0015 |
| *Pseudomonas aeruginosa* | – | – | 17 | 0.10 | 33 | 0.0025 |
| *Salmonella enteritidis* | 10 | 0.75 | 22 | 0.01 | 28 | 0.0011 |
| *Salmonella typhi* | – | | 29 | 0.01 | 35 | 0.0006 |
| *Shigella flexneri* | – | – | 21 | 0.10 | 33 | 0.0018 |
| *Staphylococcus aureus* | – | – | 19 | 0.15 | 26 | 0.0014 |
| *Staphylococcus epidermitis* | 14 | 0.36 | 29 | 0.01 | 32 | 0.0021 |

IZ = Inhibition zone (mm); Std. Imipenem; MIC: mg/ml

**Table 2** IZ and MIC of extract, AgNPs and standard against different fungal strains.

| Test microorganisms | Crude extract | | AgNPs | | Antibiotic | |
|---|---|---|---|---|---|---|
| | IZ | MIC | IZ | MIC | IZ | MIC |
| *Alternaria alternata* | 50 | 0.51 | 80 | 0.10 | 100 | 0.0001 |
| *Aspergillus flavus* | – | – | – | – | 100 | 0.0015 |
| *Aspergillus niger* | 30 | 0.82 | 50 | 0.21 | 100 | 0.0035 |
| *Aspergillus terreus* | – | – | 30 | 0.91 | 100 | 0.0002 |
| *Candida albicans* | – | – | 45 | 0.14 | 100 | 0.0025 |
| *Candida glabrata* | – | – | – | – | 100 | 0.0025 |
| *Fusarium solani* | 40 | 0.70 | 75 | 0.02 | 100 | 0.0018 |
| *Microsporum canis* | 50 | 0.53 | 90 | 0.01 | 100 | 0.0001 |
| *Trichophyton longifusis* | – | – | – | – | 100 | 0.0009 |

IZ = Inhibition zone (%); Std. Miconazole; MIC: mg/ml

highly significant activity ($P < 0.001$; 45.36%) was observed at 10 mg/kg dose at 5 h of drug treatment.

Inflammatory reactions are biphasic in nature triggered by a variety of noxious agents. The first phase of inflammation is accompanied by the release of histamine and serotonin and it persist for about 2 hrs. The second phase is mediated by the release of prostaglandin, bradykinin and lysosome and may last for 5 hrs post carrageenan injection (Koeberle, and Werz, 2018). Most of the available anti-inflammatory agents are clinically effective in blocking the later phase of inflammation (Dinarello, 2010). In present study, AgNPs produced highly significant effect at both stages of inflammation particularly at 20 mg/kg dose. Suppression of both phases of inflammation may be due to the ability of AgNPs to effectively inhibit the activity or release of different mediators involved in inflammation.

### 3.6.2. In-vitro COX-2 and 5-LOX assays

In both assays, AgNPs exhibited concentration dependent inhibition of *COX-2* and *5-LOX* enzymes (Fig. 4A & 4B). The $IC_{50}$ values of AgNPs were 15.3 and 23.01 µg/ml, as compared to that of standards Celecoxib (11.64 µg/ml) and Montelukast (17.63 µg/ml) for *COX-2* and *5-LOX* enzymes, respectively. The $IC_{50}$ values of crude extract against the stated enzymes were 29.58 µg/ml and 35.85 µg/ml, respectively. The *In-vivo* and *In-vitro* anti-inflammatory activities are in good agreement with the traditional medicinal use of *D. indica* in inflammatory disorders.

The cyclooxygenase and lipoxygenase group of enzymes play a vital role in inflammatory response. Leukotrienes, bradykinin, and prostaglandins are some of the major inflammatory mediators involved in different associated signs and symptoms (Chao et al., 2018; Rho et al., 2020). Therefore, inhibition of synthesis of these mediators is considered as an important therapeutic strategies in the effective management of inflammatory disorders. AgNPs exhibited significant inhibition against both COX-2 and 5-LOX enzymes and therefore can be considered for the development of potent anti-inflammatory drugs.

### 3.7. Analgesic activity

The crude extract and AgNPs showed significant analgesic activity at all tested doses (Table 4) however, the effect was more pronounced at 60 min of total study duration. The crude extract exhibited highest percent inhibition (34.09%; $P < 0.01$) at 200 mg/kg dose while AgNPs showed their highest inhibition (54.24%; $P < 0.001$) at 20 mg/kg dose. Similarly, the percent inhibition for AgNPs was 21.06 and 33.14% at 5 and 10 mg/kg dose, respectively. The standard tramadol exhibited maximum inhibition (59.91%) at 60 min. of pain induction. These results show that AgNPs possess analgesic activity comparable to that of standard; and that too at lower doses. Therefore, AgNPs can be used in the formulation of potentially effective and safe therapy.

**Table 3** Anti-inflammatory effect of extract, AgNPs and diclofenac on paw edema induced by carrageenan in mice.

| Groups | Mean change in the hind paw volume (ml) | | | | |
|---|---|---|---|---|---|
| | Dose (mg/kg) | BV | 1 h | 3 h | 5 h |
| Control | – | 0.09 ± 0.020 | 0.246 ± 0.001 | 0.245 ± 0.001 | 0.242 ± 0.001 |
| Extract | 50 | 0.1 ± 0.030 | 0.221 ± 0.004[a] (10.16%)[d] | 0.198 ± 0.025[a] (19.18%) | 0.188 ± 0.005[a] (22.31%) |
| | 100 | 0.09 ± 0.020 | 0.198 ± 0.007[a] (19.51) | 0.180 ± 0.006[a] (26.53) | 0.165 ± 0.007[b] (31.81) |
| | 200 | 0.1 ± 0.020 | 0.180 ± 0.006[b] (26.82) | 0.150 ± 0.002[b] (38.77) | 0.131 ± 0.002[c] (45.86) |
| AgNPs | 5 | 0.1 ± 0.020 | 0.199 ± 0.005[a] (19.10%) | 0.175 ± 0.005[a] (28.57%) | 0.158 ± 0.005[b] (34.71%) |
| | 10 | 0.09 ± 0.020 | 0.181 ± 0.006[b] (26.42%) | 0.149 ± 0.006[b] (39.18%) | 0.135 ± 0.007[c] (44.21%) |
| | 20 | 0.1 ± 0.020 | 0.159 ± 0.007[c] (35.36%) | 0.131 ± 0.005[c] (46.53%) | 0.108 ± 0.005[c] (55.37%) |
| Diclofenac | 20 | 0.09 ± 0.020 | 0.123 ± 0.005[c] (50.0%) | 0.095 ± 0.025[c] (61.22%) | 0.070 ± 0.003[c] (71.07%) |

Values are expressed as mean ± SEM (n = 5) analyzed by one way ANOVA followed by Dunnet post hoc test using Graph Pad Prism 5; BV = basal volume; [c]P ≤ 0.001, [b]P ≤ 0.01, [a]P ≤ 0.05 [d]Each value in parentheses indicate the percent inhibition.

**Table 4** Analgesic effect of various doses of extract, AgNPs and Tramadol on thermal induction of pain stimulus in mice.

| Groups | Dose (mg/kg) | 30 min | 60 min | 90 min |
|---|---|---|---|---|
| Control | – | 8.67 ± 0.22 | 9.72 ± 0.34 | 10.09 ± 0.41 |
| Extract | 50 | 10.80 ± 0.32 (9.98%)[d] | 13.4 ± 0.55[a] (18.30%) | 13.10 ± 0.22 (14.54%) |
| | 100 | 12.90 ± 0.32 (19.83%) | 15.20 ± 0.41[a] (27.72%) | 14.62 ± 0.55 (22.81%) |
| | 200 | 15.23 ± 0.66[b] (30.61%) | 16.60 ± 0.44[b] (34.09%) | 15.04 ± 0.50[a] (24.54%) |
| AgNPs | 5 | 12.11 ± 0.55 (16.13%) | 13.99 ± 0.45[a] (21.06%) | 13.00 ± 0.51 (14.26%) |
| | 10 | 13.46 ± 0.41[b] (22.46%) | 16.44 ± 0.50[b] (33.14%) | 14.38 ± 0.50[a] (21.55%) |
| | 20 | 15.84 ± 0.28[c] (33.61%) | 20.72 ± 0.66[c] (54.24%) | 18.29 ± 0.58[c] (41.19%) |
| Tramadol | 30 | 20.31 ± 0.78[c] (54.57%) | 21.87 ± 0.50[c] (59.91%) | 21.88 ± 0.70[c] (59.22%) |

Values are expressed as mean ± SEM (n = 5) analyzed by one way ANOVA followed by Dunnet post hoc test using Graph Pad Prism 5; [c]P ≤ 0.001, [b]P ≤ 0.01, [a]P ≤ 0.05. [d]Each value in parentheses indicate the percent inhibition.

### *3.8. Muscle relaxant activity*

In both tests, *D. indica* crude extract showed significant effect ($P < 0.05$) at all studied doses and the effect was more pronounced ($P < 0.01$) at 60 and 90 min of study duration (Table 5). Similarly, AgNPs demonstrated significant ($P < 0.05$) muscle relaxant effect at all studied doses however; maximum relaxation ($P < 0.01$) was produced after 60 and 90 min of drug administration. The standard diazepam produced significant muscle relaxation at 0.25 mg/kg throughout the study in both tests. The present results suggests that AgNPs possess excellent relaxant activity comparable to crude aqueous extract and that too at much lower doses.

Musculoskeletal problems require the combined use of NSAIDs and muscle relaxants because pain is mostly associated with muscle stretching (Gong et al., 2013; Malanga, and Wolff, 2008). For such conditions, *D. indica* extract has been widely used as a single therapy agent in the Ayurvedic system. Therefore, the use of its silver NPs, is very much advantageous than prescribing combination of synthetic drugs for musculoskeletal disorders. Furthermore, silver itself is usually used for various joint pain conditions (Zajonz et al., 2017). This

**Table 5** Effect of various doses of extract, AgNPs and diazepam on muscle relaxation (chimney test and traction test).

| Group | Dose (mg/kg) | Chimney test (%) | | | Traction test (%) | | |
|---|---|---|---|---|---|---|---|
| | | 30 min | 60 min | 90 min | 30 min | 60 min | 90 min |
| Diazepam | 0.25 | 100 ± 0.00[a] | 100 ± 0.00[a] | 100 ± 0.00[a] | 100 ± 0.00[a] | 100 ± 0.00[a] | 100 ± 0.00[a] |
| Extract | 50 | 37.45 ± 1.32[b] | 53.62 ± 1.11[a] | 53.07 ± 1.08[a] | 41.12 ± 02.76[b] | 52.00 ± 1.80[a] | 52.11 ± 1.99[a] |
| | 100 | 41.78 ± 1.88[b] | 58.32 ± 1.53[a] | 58.01 ± 1.98[a] | 43.88 ± 1.05[b] | 54.71 ± 1.08[a] | 52.62 ± 2.11[a] |
| | 200 | 51.12 ± 2.23[b] | 62.43 ± 2.71[a] | 61.11 ± 2.99[a] | 43.66 ± 1.00[b] | 57.00 ± 2.22[a] | 57.32 ± 2.98[a] |
| AgNPs | 5 | 42.03 ± 2.86[b] | 49.07 ± 1.77[a] | 48.00 ± 1.77[a] | 44.07 ± 0.12[b] | 49.80 ± 2.89[a] | 49.70 ± 2.10[a] |
| | 10 | 56.06 ± 2.11[a] | 63.37 ± 1.61[a] | 63.80 ± 2.01[a] | 48.78 ± 1.66[b] | 58.03 ± 1.98[a] | 57.60 ± 1.98[a] |
| | 20 | 67.12 ± 2.98[a] | 71.23 ± 2.80[a] | 71.01 ± 2.00[a] | 51.00 ± 1.00[b] | 61.10 ± 1.95[a] | 59.08 ± 2.11[a] |

Data presented as mean ± S.E.M, (n = 5). ANOVA followed by Dunnett's post hoc test.
[a] P < 0.01.
[b] P < 0.05.

added advantage of AgNPs greatly promotes its use as alternative herbal therapy for safe and effective management of different pain conditions.

## 4. Conclusions

This study reports a safe and rapid method for the green synthesis and characterization of AgNPs using *D. indica* root extract. The NPs were mostly in the size of 17–55 nm. *UV–Vis* spectra confirmed the biosynthesis of AgNPs; SEM and TEM analysis revealed their spherical shape while FT-IR spectra confirmed the involvement of various phytochemicals in their reduction and capping.

The synthesized AgNPs showed significant antibacterial activity against *S. typhi* and *S. epidermidis* as compared to standard Imipenem. Among fungal strains silver NPs demonstrated maximum activity against *M. canis* and *F. solani*. AgNPs also showed significant anti-inflammatory activity comparable to that of standard in both *In-vivo* and *In-vitro* models. Similarly they also showed considerable analgesic and muscle relaxant activities. Results of the study suggest that these AgNPs can be studied further for the development of more effective and safe formulations.

## CRediT Author statement

"I.H. and F.K. conceived and designed the experiments; I.H., F.K., R.U. and Z.U. performed the experiments; S.M.U.K, S. A., A.S.D., A.K. and A.A.K.K. analyzed the data; S.M.U.K, S.A. and F.K. contributed reagents and materials; All the authors contributed equally in the paper write up, review and approved the final draft.

## Declaration of Competing Interest

The authors declare no competing interest of any kind in this work.

## Acknowledgements

The authors are grateful to the University of Peshawar for providing research facilities and Prof. Dr. Muhammad Ibrar, Department of Botany, University of Peshawar for plant authentication.

## Author contributions

"I.H. and F.K. conceived and designed the experiments; I.H., F.K., R.U. and Z.U. performed the experiments; S.M.U.K, S. A., A.S.D., A.K. and A.A.K.K. analyzed the data; S.M.U.K, S.A. and F.K. contributed reagents and materials; All the authors contributed equally in the paper write up, review and approved the final draft.

## Appendix A. Supplementary material

Supplementary data to this article can be found online at https://doi.org/10.1016/j.arabjc.2021.103110.

## References

Ahmad, A., Wei, Y., Ullah, S., Shah, S.I., Nasir, F., Shah, A., Iqbal, Z., Tahir, K., Khan, U.A., Yuan, Q., 2017. Synthesis of phytochemicals-stabilized gold nanoparticles and their biological activities against bacteria and Leishmania. Microb. Pathog. 110, 304–312. https://doi.org/10.1016/j.micpath.2017.07.009.

Ahmad, H., Venugopal, K., Rajagopal, K., De Britto, S., Nandini, B., Pushpalatha, H.G., Konappa, N., Udayashankar, A.C., Geetha, N., Jogaiah, S., 2020. Green synthesis and characterization of zinc oxide nanoparticles using Eucalyptus globules and their fungicidal ability against pathogenic fungi of apple orchards. Biomolecules 10, 425. https://doi.org/10.3390/biom10030425.

Al-Radadi, N.S., 2019. Green synthesis of platinum nanoparticles using Saudi's Dates extract and their usage on the cancer cell treatment. Arab. J. Chem. 12 (3), 330–349. https://doi.org/10.1016/j.arabjc.2018.05.008.

Algebaly, A.S., Mohammed, A.E., Abutaha, N., Elobeid, M.M., 2020. Biogenic synthesis of silver nanoparticles: antibacterial and cytotoxic potential. Saudi J. Biol. Sci. 27 (5), 1340–1351. https://doi.org/10.1016/j.sjbs.2019.12.014.

Biziere, K., Bourguignon, J., Chambon, J., Heaulme, M., Perio, A., Tebib, S., Wermuth, C., 1987. A 7-phenyl substituted triazolopyridazine has inverse agonist activity at the benzodiazepine receptor site. Br. J. Pharmacol. 90, 183–190. htpps://doi.org/10.1111/j.1476-5381.1987.tb16839.

Boyanova, L., Gergova, G., Nikolov, R., Derejian, S., Lazarova, E., Katsarov, N., Mitov, I., Krastev, Z., 2005. Activity of Bulgarian propolis against 94 Helicobacter pylori strains in vitro by agar-well diffusion, agar dilution and disc diffusion methods. J. Med. Microbiol. 54, 481–483. https://doi.org/10.1099/jmm.0.45880-0.

Chao, H., Liu, Y., Lin, C., Xu, X., Li, Z., Bao, Z., Fan, L., Tao, C., Zhao, L., Liu, Y., Wang, X., You, Y., Liu, N., Ji, J., 2018. Activation of bradykinin B2 receptor induced the inflammatory responses of cytosolic phospholipase A2 after the early traumatic brain injury. Biochim. Biophys. Acta. Mol. Basis. Dis. 1864 (9), 2957–2971. https://doi.org/10.1016/j.bbadis.2018.06.006.

Dinarello, C.A., 2010. Anti-inflammatory agents: present and future. Cell 140 (6), 935–950. https://doi.org/10.1016/j.cell.2010.02.043.

Fazli, K., Iqbal, Z., Khan, A., Zaki, U., Nasir, F., 2012. Validation of Some of the ethnopharmacological uses of xanthium strumarium and duchesnea indica. Pak. J. Bot. 44, 1199–1201.

Fazli, K., Iqbal, Z., Khan, A., Zaki, U., Nasir, F., Iqbal, Z., Khan, A., Shah, Y., Ahmad, L., Nasir, F., Hassan, M., Shah, W.A., Shah, W., 2014. Evaluation of anti-inflammatory activity of selected medicinal plants of Khyber Pakhtunkhwa. Pakistan. Pak. J. Pharm. Sci 27, 365–368.

Feng, Q.L., Wu, J., Chen, G.Q., Cui, F.Z., Kim, T.N., Kim, J.O., 2000. A mechanistic study of the antibacterial effect of silver ions on *Escherichia coli* and *Staphylococcus aureus*. J. Biomed. Mater. 52 (4), 662–668. https://doi.org/10.1002/(ISSN)1097-463610.1002/1097-4636(20001215)52:4<>1.0.CO;2-U10.1002/1097-4636(20001215)52:4<662::AID-JBM10>3.0.CO;2-3.

Geetha, N., Bhavya, G., Abhijith, P., Shekhar, R., Dayananda, K., Jogaiah, S., 2021. Insights into nanomycoremediation: Secretomics and mycogenic biopolymer nanocomposites for heavy metal detoxification. J. Hazard. Mater. 409, 124541. https://doi.org/10.1016/j.jhazmat.2020.124541.

Gong, L., Dong, J.-Y., Li, Z.-R., 2013. Effects of combined application of muscle relaxants and celecoxib administration after total knee arthroplasty (TKA) on early recovery: a randomized, double-blind, controlled study. J. Arthroplasty. 28 (8), 1301–1305. https://doi.org/10.1016/j.arth.2012.10.002.

Hu, W., Han, W., Huang, C., Wang, M.-H., 2011. Protective effect of the methanolic extract from Duchesnea indica against oxidative stress in vitro and in vivo. Environ. Toxicol. Pharmacol. 31 (1), 42–50. https://doi.org/10.1016/j.etap.2010.09.004.

Islam, N.U., Jalil, K., Shahid, M., Muhammad, N., Rauf, A., 2019. Pistacia integerrima gall extract mediated green synthesis of gold nanoparticles and their biological activities. Arab. J. Chem. 12 (8), 2310–2319. https://doi.org/10.1016/j.arabjc.2015.02.014.

Jogaiah, S., Kurjogi, M., Abdelrahman, M., Hanumanthappa, N., Tran, L.-S., 2019. Ganoderma applanatum-mediated green synthesis of silver nanoparticles: Structural characterization, and in vitro and in vivo biomedical and agrochemical properties. Arab. J. Chem. 12 (7), 1108–1120. https://doi.org/10.1016/j.arabjc.2017.12.002.

Joshi, S.M., De Britto, S., Jogaiah, S., 2021. Myco-engineered selenium nanoparticles elicit resistance against tomato late blight disease by regulating differential expression of cellular, biochemical and defense responsive genes. J. Biotechnol. 325, 196–206. https://doi.org/10.1016/j.jbiotec.2020.10.023.

Koeberle, A., Werz, O., 2018. Natural products as inhibitors of prostaglandin E2 and pro-inflammatory 5-lipoxygenase-derived lipid mediator biosynthesis. Biotechnol. Adv. 36 (6), 1709–1723. https://doi.org/10.1016/j.biotechadv.2018.02.010.

Lim, J.K., Liu, T., Jeong, J., Shin, H., Jang, H.J., Cho, S.-P., Park, J. S., 2020. In situ syntheses of silver nanoparticles inside silver citrate nanorods via catalytic nanoconfinement effect. Colloids Surf, A Physicochem. Eng. Asp. 605, 125343. https://doi.org/10.1016/j.colsurfa.2020.125343.

Lingadurai, S., Nath, L.K., Kar, P.K., Besra, S.E., Joseph, R.V., 2007. Anti-inflammatory and anti-nociceptive activities of methanolic extract of the leaves of Fraxinus floribunda Wallich. Afr. J. Tradit. Complement. Altern. Med. 4, 411–416.

Luo, S., Guo, L., Sheng, C., Zhao, Y., Chen, L., Li, C., Jiang, Z., Tian, H., 2020. Rapid identification and isolation of neuraminidase inhibitors from mockstrawberry (Duchesnea indica Andr.) based on ligand fishing combined with HR-ESI-Q-TOF-MS. Acta Pharm. Sin. B. 10 (10), 1846–1855. https://doi.org/10.1016/j.apsb:2020.04.001.

Malanga, G., Wolff, E., 2008. Evidence-informed management of chronic low back pain with nonsteroidal anti-inflammatory drugs, muscle relaxants, and simple analgesics. Spine J. 8 (1), 173–184. https://doi.org/10.1016/j.spinee.2007.10.013.

Mathew, S., Victório, C.P., Sidhi, M.S., B.H, B.T., 2020. Biosynthesis of silver nanoparticle using flowers of Calotropis gigantea (L.) W. T. Aiton and activity against pathogenic bacteria. Arab. J. Chem. 13, 9139–9144. https://doi.org/10.1016/j.arabjc.2020.10.038.

Nandini, B., Puttaswamy, H., Prakash, H.S., Adhikari, S., Jogaiah, S., Nagaraja, G., 2020. Elicitation of novel trichogenic-lipid nanoemulsion signaling resistance against pearl millet downy mildew disease. Biomolecules. 10, 25. https://doi.org/10.3390/biom10010025.

Okur, M.E., Karadağ, A.E., Özhan, Y., Sipahi, H., Ayla, Ş., Daylan, B., Kültür, Ş., Demirci, B., Demirci, F., 2021. Anti-inflammatory, analgesic and in vivo-in vitro wound healing potential of the Phlomis rigida Labill. extract. J. Ethnopharmacol. 266, 113408. https://doi.org/10.1016/j.jep.2020.113408.

Olomola, T.O., Mphahlele, M.J., Gildenhuys, S., 2020. Benzofuran-selenadiazole hybrids as novel α-glucosidase and cyclooxygenase-2 inhibitors with antioxidant and cytotoxic properties. Bioorg. Med. Chem. 100, 103945. https://doi.org/10.1016/j.bioorg.2020.103945.

Oprica, L., Andries, M., Sacarescu, L., Popescu, L., Pricop, D., Creanga, D., Balasoiu, M., 2020. Citrate-silver nanoparticles and their impact on some environmental beneficial fungi. Saudi J. Biol. Sci. 27 (12), 3365–3375. https://doi.org/10.1016/j.sjbs.2020.09.004.

Oves, M., Arshad, M., Khan, M.S., Ahmed, A.S., Azam, A., Ismail, Iqbal M.I., 2015. Anti-microbial activity of cobalt doped zinc oxide nanoparticles: Targeting water borne bacteria. J. Saudi Chem. 19 (5), 581–588. https://doi.org/10.1016/j.jscs.2015.05.003.

Patil, S.P., 2020. Ficus carica assisted green synthesis of metal nanoparticles: a mini review. Biotechnol Rep. 28, e00569. https://doi.org/10.1016/j.btre.2020.e00569.

Ponsanti, K., Tangnorawich, B., Ngernyuang, N., Pechyen, C., 2020. A flower shape-green synthesis and characterization of silver nanoparticles (AgNPs) with different starch as a reducing agent. J. Mater. Res. 9 (5), 11003–11012. https://doi.org/10.1016/j.jmrt.2020.07.077.

Punjabi, K., Mehta, S., Chavan, R., Chitalia, V., Deogharkar, D., Deshpande, S., 2018. Efficiency of biosynthesized silver and zinc nanoparticles against multi-drug resistant pathogens. Front. microbiol. 9, 2207. https://doi.org/10.3389/fmicb.2018.02207.

Qiao, W., Yao, Z., Zhang, W., Duan, H.Q., 2009. Two new triterpenes from Duchesnea indica. Chin. Chem. Lett. 20 (5), 572–575. https://doi.org/10.1016/j.cclet.2008.12.052.

Rana, A., Yadav, K., Jagadevan, S., 2020. A comprehensive review on green synthesis of nature-inspired metal nanoparticles: mechanism, application and toxicity. J. Clean. Prod. 272, 122880. https://doi.org/10.1016/j.jclepro.2020.122880.

Rho, T., Jeong, H.W., Hong, Y.D., Yoon, K., Cho, J.Y., Yoon, K.D., 2020. Identification of a novel triterpene saponin from Panax ginseng seeds, pseudoginsenoside RT8, and its antiinflammatory activity. J. Ginseng Res. 44 (1), 145–153. https://doi.org/10.1016/j.jgr.2018.11.001.

Robles-Martínez, M., González, J.F.C., Pérez-Vázquez, F.J., Montejano-Carrizales, J.M., Pérez, E., Patiño-Herrera, R., 2019. Antimycotic activity potentiation of Allium sativum extract and silver nanoparticles against Trichophyton rubrum. Chem. Biodivers. 16 (4). https://doi.org/10.1002/cbdv.v16.410.1002/cbdv.201800525.

Sharma, D.., Shandilya, P., Saini, N.K., Singh, P., Thakur, V.K., Saini, R.V., Mittal, D., Chandan, G., Saini, V., Saini, A.K., 2021. Insights into the synthesis and mechanism of green synthesized antimicrobial nanoparticles, answer to the multidrug resistance. Mater. Today Chem. 19, 100391. https://doi.org/10.1016/j.mtchem.2020.100391.

Sondi, I., Salopek-Sondi, B., 2004. Silver nanoparticles as antimicrobial agent: a case study on E. coli as a model for Gram-negative bacteria. J. Colloid Interface Sci. 275, 177–182. htpp://doi.org/10.1016/j.jcis.2004.02.012.

Tailor, G., Yadav, B.L., Chaudhary, J., Joshi, M., Suvalka, C., 2020. Green synthesis of silver nanoparticles using Ocimum canum and their anti-bacterial activity. Biochem. Biophys. Rep. 24, 100848. https://doi.org/10.1016/j.bbrep.2020.100848.

Villar, R., Laguna, M., Calleja, J., Cadavid, I., 1992. Effects of Skeletonema costatum extracts on the central nervous system. Planta med. 58 (05), 398–404. https://doi.org/10.1055/s-2006-961500.

Winter, C.A., Risley, E.A., Nuss, G.W., 1962. Carrageenin-induced Edema in hind paw of the rat as an assay for antiinflammatory drugs. Proc. Soc. Exp. Biol. Med. 111 (3), 544–547. https://doi.org/10.3181/00379727-111-27849.

Yang, W., Ho, Y.C., Tang, C.M., Hsieh, Y.S., Chen, P.N., Lai, C.T., Yang, S.F., Lin, C.W., 2019. Duchesnea indica extract attenuates oral cancer cells metastatic potential through the inhibition of the matrix metalloproteinase-2 activity by down-regulating the MEK/ERK pathway. Phytomedicine 63, 152960. https://doi.org/10.1016/j.phymed.2019.152960.

Zajonz, D., Birke, U., Ghanem, M., Prietzel, T., Josten, C., Roth, A., Fakler, J.K., 2017. Silver-coated modular Megaendoprostheses in salvage revision arthroplasty after periimplant infection with extensive bone loss–a pilot study of 34 patients. BMC Musculoskelet Disord. 18, 1–7. https://doi.org/10.1186/s12891-017-1742-7.

Zhao, L., Zhang, S.L., Tao, J.Y., Jin, F., Pang, R., Guo, Y.J., Ye, P., Dong, J.H., Zheng, G.H., 2008. Anti-inflammatory mechanism of a folk herbal medicine, Duchesnea indica (Andr) Focke at RAW264.7 cell line. Immunol. Invest. 37 (4), 339–357. https://doi.org/10.1080/08820130802111589.